

MFE revisited, Part 1: Adaptive Grid-Generation using the Heat Equation

PAUL A. ZEGELING
*Mathematical Institute
University of Utrecht
Utrecht, the Netherlands*

Abstract

In this paper the moving-finite-element method (MFE) is used to solve the heat equation, with an artificial time component, to give a non-uniform (steady-state) grid that is adapted to a given profile. It is known from theory and experiments that MFE, applied to parabolic PDEs, gives adaptive grids which satisfy an equidistribution type law. This property is used to create non-uniform finite-element grids that are dictated by second-order derivatives of the solution. The proposed procedure could be used to create an initial grid for MFE itself, to define a regridding strategy for MFE in case of a distorted grid, or to prescribe a new adaptive grid method where the heat equation is used as a "monitor function".

Keywords: Moving grids, partial differential equations, finite elements, method of lines, equidistribution

1 Introduction

Moving grids, and moving-finite-elements (MFE) ([1, 3, 4, 6, 7]) in particular, have successfully been used to numerically solve time-dependent partial differential equation (PDE) models in one and two space dimensions. The one-dimensional case has indicated both theoretically and experimentally that MFE applied to parabolic equations produces non-uniform equidistributed grids with a weight function depending on first and second order derivatives of the PDE solution. In two space dimensions, where no theory is available on MFE and its relation with equidistribution, numerical experiments have shown that, when MFE is applied to parabolic PDEs, the grid points are positioned in regions where second order derivatives are large. In this paper that property is used to create non-uniform finite-element grids that are dictated by second-order derivatives of the solution. First, the relation between MFE and equidistribution is explained. Then it is shown how to take advantage of this property using a specific PDE, viz. the heat equation with a time- and space-dependent sourceterm. Finally, this procedure is applied in numerical experiments both in one and two space dimensions for different types of functions.

2 MFE and equidistribution

Consider the following time-dependent PDE in n space dimensions

$$\frac{\partial u}{\partial t} = \delta \Delta u - \beta \cdot \nabla u + S := \mathcal{L}(u), \quad (1)$$

for $\underline{x} \in \Omega \subset \mathbb{R}^n$, $t > 0$ with given boundary conditions on $\partial\Omega$ and initial condition for $t = 0$ (the cases $n = 1$ and $n = 2$ will be treated in the numerical experiments).

Approximate the PDE solution by

$$u \approx U = \sum_{j=1}^M U_j(t) \alpha_j(\underline{x}, \{\underline{X}_j(t)\}), \quad (2)$$

where M denotes the total number of grid points, and α_j are piecewise linear ‘hat’ functions on a time-dependent grid $\{\underline{X}_j(t)\}$.

Differentiating with respect to time t by the chain rule and using the time-dependence of the grid points $(X_{1,j}(t), \dots, X_{n,j}(t))$ we obtain

$$U_t = \sum_{j=1}^M \{\dot{U}_j \alpha_j + \sum_{l=1}^n \dot{X}_{l,j} \gamma_{l,j}\}. \quad (3)$$

Note that the basis functions $\gamma_{l,j}$ have the same support as α_j . The equations determining the semi-discrete unknowns U_j , $X_{1,j}$, ..., $X_{n,j}$ are obtained by minimizing the PDE residual \mathcal{R} w.r.t. \dot{U}_j , $\dot{X}_{1,j}$, ..., $\dot{X}_{n,j}$, where

$$\mathcal{R} := \|U_t - \mathcal{L}(U)\|_{L_2(\Omega)}^2 + \mathcal{P}^2. \quad (4)$$

The second term \mathcal{P}^2 is a regularization term containing small parameters ϵ_1^2 and ϵ_2^2 to prevent the parametrization (3) from becoming degenerate (for more details see [6]). The minimization yields the implicit stiff ODE system

$$\mathcal{M}(\eta, \epsilon_1^2) \dot{\eta} = H(\eta, \epsilon_2^2, \delta), \quad (5)$$

with an initial vector $\eta(0)$ containing the initial solution and the initial grid. In (5) \mathcal{M} is an extended mass-matrix, which is regular for $\epsilon_1^2 > 0$. This semi-discrete ODE system can be solved with a stiff ODE solver.

For $n = 1$, it can be shown, that the grid points in the semi-discrete equations (5) in the limit ($M \rightarrow \infty$) satisfy

$$\dot{x} = \beta + \delta \left[2 \frac{u_{xxx}}{u_{xx}} - 3 \frac{\xi_{xx}}{\xi_x} \right], \quad (6)$$

where ξ is a transformed space variable (see e.g. [5]). In steady-state situations it can be derived from (6) that the grid is equidistributed according to the rule $(x_\xi W)_\xi = 0$, with a weightfunction $W = |u_x|^{1/3} |u_{xx}|^{2/3}$. Without convection terms ($\beta = 0$) this reduces to $W = |u_{xx}|^{2/3}$, which indicates that grid points are expected to be concentrated in regions of large second derivatives.

In contrast with the 1D situation no theory is available to predict such an ‘equidistributional’ behaviour in the two dimensional case. However, it is conjectured that for $n = 2$, without regularization terms (i.e. with $\epsilon_1^2 = \epsilon_2^2 = 0$), the grid movement satisfies

$$\dot{x} = \beta_1 + \delta \phi_1, \quad (7)$$

$$\dot{y} = \beta_2 + \delta \phi_2, \quad (8)$$

with functions ϕ_1 and ϕ_2 depending on spatial derivatives. In the next section we will examine the $\beta = (0, 0)^T$ case, i.e. first order derivatives are omitted.

3 Generating adaptive grids with the heat equation

In this section we will describe a way to generate adaptive grids with MFE applied to the heat equation plus sourceterm.

Consider the spatial domain $\Omega = [0, 1]^n \in \mathbb{R}^n$ and an artificial time variable $\theta \geq 0$. Assuming that a function $u^\infty(\underline{x}) \in C^2(\bar{\Omega})$ is given, we define, for $\underline{x} \in \Omega$ and $\theta \in [0, \Theta]$, the function $u^*(\underline{x}, \theta) = [1 - e^{-\lambda\theta}] u^\infty(\underline{x})$, where λ is a positive parameter and Θ is the end point of time.

Consider the heat equation

$$\frac{\partial u}{\partial \theta} = \delta \Delta u + \mathcal{F}, \quad (9)$$

with diffusion coefficient $\delta \geq 0$ and (time-dependent) boundary and initial conditions

$$u|_{\partial\Omega} = u^*|_{\partial\Omega} \equiv [1 - e^{-\lambda\theta}] u^\infty|_{\partial\Omega}, \quad (10)$$

$$u|_{\theta=0} = u^*|_{\theta=0} \equiv 0. \quad (11)$$

If we define the sourceterm \mathcal{F} in (9) as

$$\mathcal{F}(\underline{x}, \theta) = \lambda u^\infty(\underline{x}) e^{-\lambda\theta} - \delta [1 - e^{-\lambda\theta}] \Delta u^\infty(\underline{x}),$$

then it is easily verified that the analytical solution of PDE model (9), (10), (11) satisfies

$$u^*(\underline{x}, \theta) = [1 - e^{-\lambda\theta}] u^\infty(\underline{x}). \quad (12)$$

A useful property of this solution, of which we will take advantage, is

$$\lim_{\theta \rightarrow \infty} u(\underline{x}, \theta) = \lim_{\theta \rightarrow \infty} u^*(\underline{x}, \theta) = u^\infty(\underline{x}).$$

Since the initial solution of the model is the *zero*-function, we could start our procedure with a uniform-grid distribution. As time evolves, we would like the grid to adapt to the final solution profile $u^\infty(\underline{x})$. To be more specific, for $\lambda = \mathcal{O}(1)$ and $\Theta \gg 1$, the relative deviation of u^* from u^∞ will be

$$\left| \frac{u^*(\underline{x}, \Theta) - u^\infty(\underline{x})}{u^\infty(\underline{x})} \right| = e^{-\lambda\Theta} \ll 1.$$

The steady-state parameter λ therefore influences the speed of reaching steady-state ($\lambda = 1$ will be the standard choice). Now applying MFE, as described in the previous section, to (9) gives (for $n = 2$), while ignoring the regularization influence, in the limit ($M \rightarrow \infty$)

$$\frac{\partial x}{\partial \theta} = \delta \phi_1, \quad (13)$$

$$\frac{\partial y}{\partial \theta} = \delta \phi_2,$$

with functions ϕ_1 and ϕ_2 , that are likely to depend on first-and second order spatial derivatives of the solution $u(\underline{x}, \theta)$. In the limit $\theta \rightarrow \infty$ (steady-state) we also have from (13):

$$\frac{\partial u}{\partial \theta} = \phi_1 = \phi_2 = 0,$$

which means: a non-uniform adaptive grid for the function $u^\infty(\underline{x})$, determined by the ‘zeroes’ of the functions ϕ_1 and ϕ_2 .

4 A numerical example in one space dimension

In this section a numerical example in 1D is given to illustrate the method of generating adaptive grids using MFE and the heat equation (9).

Example 1:

$$u^\infty(x) = \frac{1}{2} \left(1 + \tanh \left(R \left(\frac{1}{16} - \left(x - \frac{1}{2} \right)^2 \right) \right) \right).$$

In Figure 1 solutions and grids are displayed for this function. For $R = 25$ and $R = 35$ the solutions are given at $\theta = 0.01, 0.1, 0.5, 1$ and 5 ('steady-state'). The standard parameter choice $\delta = 1$, $\epsilon_1^2 = 0.1$ and $\epsilon_2^2 = 10^{-4}$ for $M = 31$ yields adaptive grids with the grid points concentrated in regions of large second order derivatives, as predicted by the 1D theory.

Figures 2, 3, and 4 show results for $R = 50$ and different values of the method parameters δ , ϵ_1^2 and ϵ_2^2 . Increasing δ corresponds to emphasizing the Laplacian in the heat equation, and therefore producing 'more adapted' grids. Lower values of δ give almost uniform grids. For $\delta \downarrow 0$, equation (13) predicts no grid movement at all.

Increasing ϵ_1^2 or ϵ_2^2 produces non-moving uniform grids, while smaller values for these two parameters yield more adaptivity, however on less smooth grids. In this respect, ϵ_1^2 and ϵ_2^2 may also be seen as 'grid-smoothing' parameters.

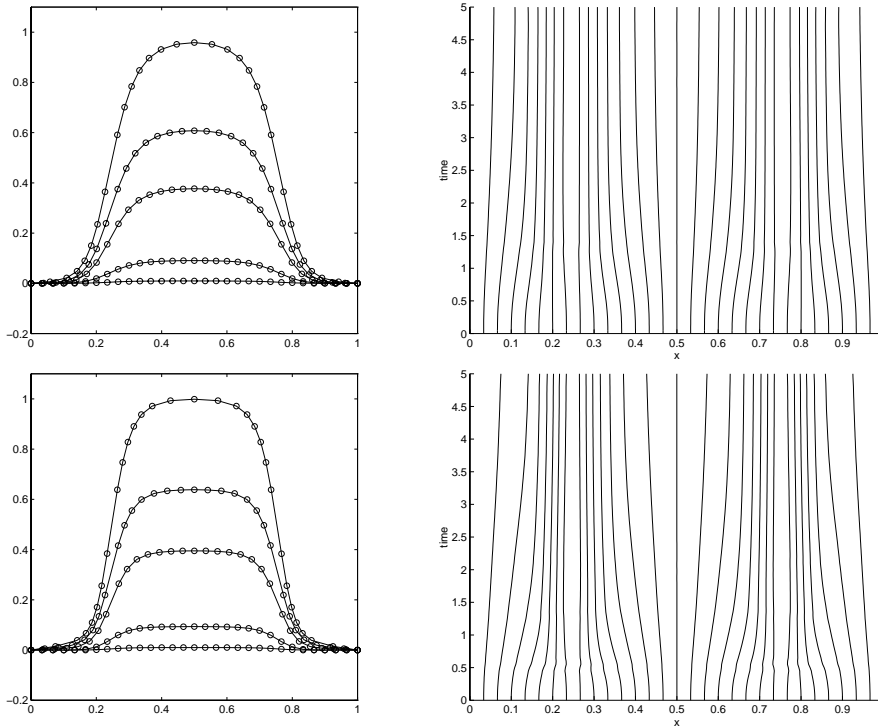


Figure 1: Solutions and grids for the 1D example.

5 Numerical examples in two space dimensions

In this section numerical examples in 2D are given to illustrate the adaptive grid procedure. In the experiments the following standard choices are made: 1. a uniform starting grid (since $u^*|_{t=0} = 0$),

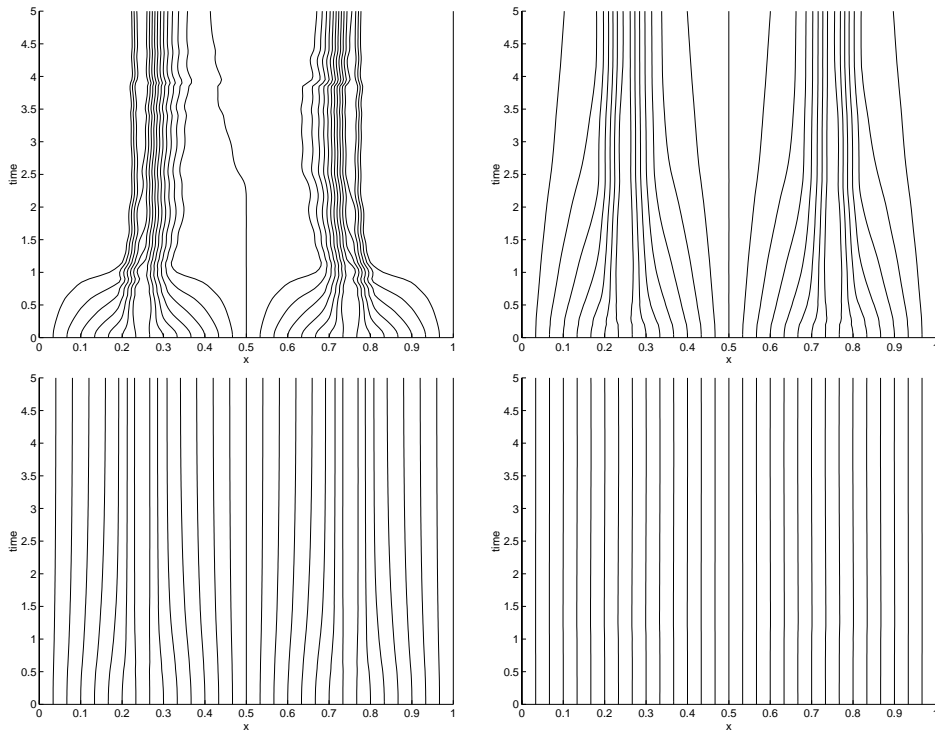


Figure 2: δ -variation for the 1D example. Values for δ are 10, 1, 0.1, and 0.001, respectively.

2. steady-state parameter $\lambda = 1$, 3. final point of time $\Theta = 100$, 4. MFE-regularization parameters $\epsilon_1^2 = 0.1$ and $\epsilon_2^2 = 1.E - 8$, and 5. adaptivity parameter $\delta = 1$.

Example 2:

$$u^\infty(x, y) = \frac{1}{2} \left(1 + \tanh \left(R \left(\frac{1}{16} - \left(x - \frac{1}{2} \right)^2 - \left(y - \frac{1}{2} \right)^2 \right) \right) \right).$$

Figure 5 shows the evolution from uniform grid at $\theta = 0$ to adaptive grid at $\theta = 100$ for $R = 35$ on a 21×21 -grid. In Figure 6 the steady-state grids and solutions (at $\theta = 100$) are displayed for this function and increasing values of R ($= 25, 35, 50, 100$) on a 29×29 grid.

Example 3:

$$u^\infty(x, y) = 2^{4m} x^m (1-x)^m y^m (1-y)^m.$$

In Figure 7 (upper two plots) the steady-state grid and solution is depicted for $m = 50$. Note the grid positioning at the top and the bottom of the sharp peak, corresponding with regions of large second order derivatives.

Example 4:

$$u^\infty(x, y) = \sum_{j=1}^p e^{-\alpha_j((x-x_j)^2+(y-y_j)^2)} + \mathcal{C} (1 - \tanh(\alpha(x - x_0)))(1 - \tanh(\alpha(y - y_0))).$$

In Figure 7 (middle two plots) the steady-state grids are shown for $p = 4$, $\alpha_1 = 200$, $\alpha_2 = 25$, $\alpha_3 = 100$, $\alpha_4 = 50$ and $\mathcal{C} = 0$ on a 29×29 grid (right), and for $p = 2$, $\alpha_1 = 100$, $\alpha_2 = 25$ and $\mathcal{C} = 0$ on a 21×21 grid (left). In the lower two plots the grid and solution for $p = 1$, $\alpha_1 = 100$ and

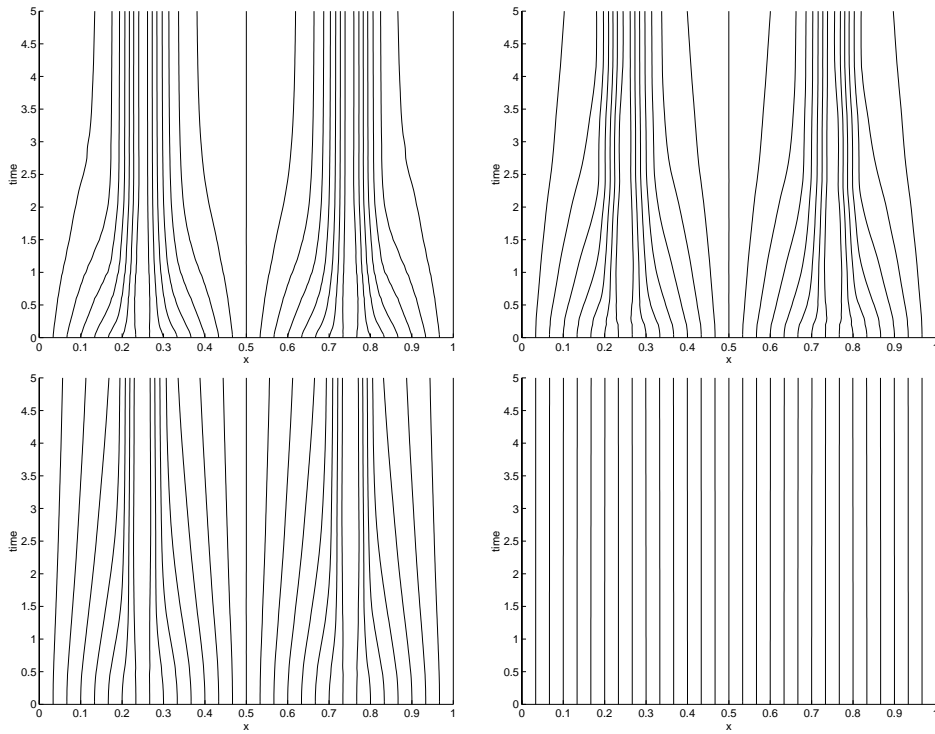


Figure 3: ϵ_1^2 -variation for the 1D example. Values for ϵ_1^2 are 10^{-4} , 0.1, 1 and 10^3 , respectively.

$C = \frac{1}{4}$, $\alpha = 50$, $x_0 = y_0 = 50$ are displayed.

Finally, in Figure 8 the effects of changing the parameters in the method are clearly observed. In this experiment the function of example 2 is used with $R = 35$ and different values for ϵ_1^2 , ϵ_2^2 and δ . Similar results are obtained as for the 1D case. The parameter δ can indeed be seen as an adaptivity parameter, while the regularization parameters ϵ_1^2 and ϵ_2^2 seem to smooth the grid.

6 Conclusions

We have constructed a way to generate solution-adaptive grids using the moving-finite-element method in combination with the heat equation.

This procedure could be used to create an initial grid for MFE itself, if the initial solution is at least twice continuously differentiable.

In a discrete manner, the procedure could define a regridding strategy in case of distorted MFE grids, or even as a procedure on its own to follow steep solutions of a PDE. Before that, the method should first be made more efficient in solving the (pseudo) steady-state equations.

It would be interesting to investigate similar procedures for the, more sophisticated, gradient-weighted case [2].

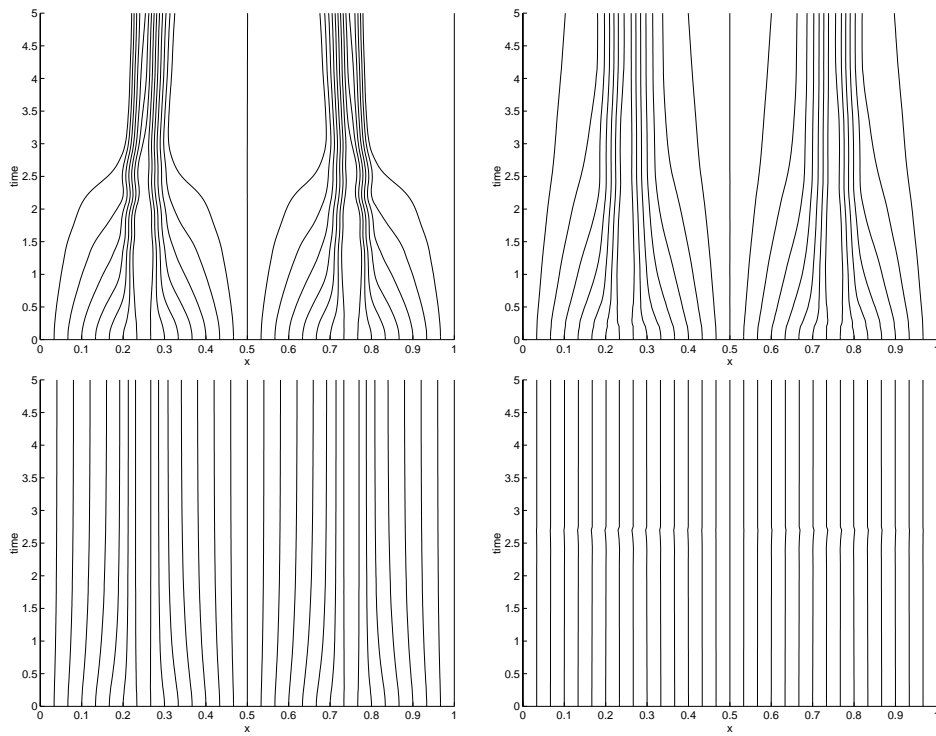


Figure 4: ϵ_2^2 -variation for the 1D example. Values for ϵ_2^2 are 10^{-5} , 10^{-4} , 10^{-3} and 0.1, respectively.

References

- [1] M.J. Baines. *Moving Finite Elements*. Clarendon Press, Oxford, 1994.
- [2] N. Carlson and K. Miller. Design and application of a gradient-weighted moving finite element code, part II, in 2D. *Technical report 237, Purdue University, 1994*.
- [3] K. Miller and R.N. Miller. Moving finite elements I. *SIAM J. Numer. Anal.*, 18:1019–1032, 1981.
- [4] K. Miller. Moving finite elements II. *SIAM J. Numer. Anal.*, 18:1033–1057, 1981.
- [5] P.A. Zegeling and J.G. Blom. A note on the grid movement induced by MFE. *Int. J. Numer. Meth. Eng.*, 35:623–636, 1992.
- [6] P.A. Zegeling. Moving-finite-element solution of time-dependent partial differential equations in two space dimensions. *Comp. Fluid Dyn.*, 1:135–159, 1993.
- [7] P.A. Zegeling. *Moving-Grid Methods for Time-Dependent Partial Differential Equations*. CWI Tract 94, CWI, Amsterdam, 1993.

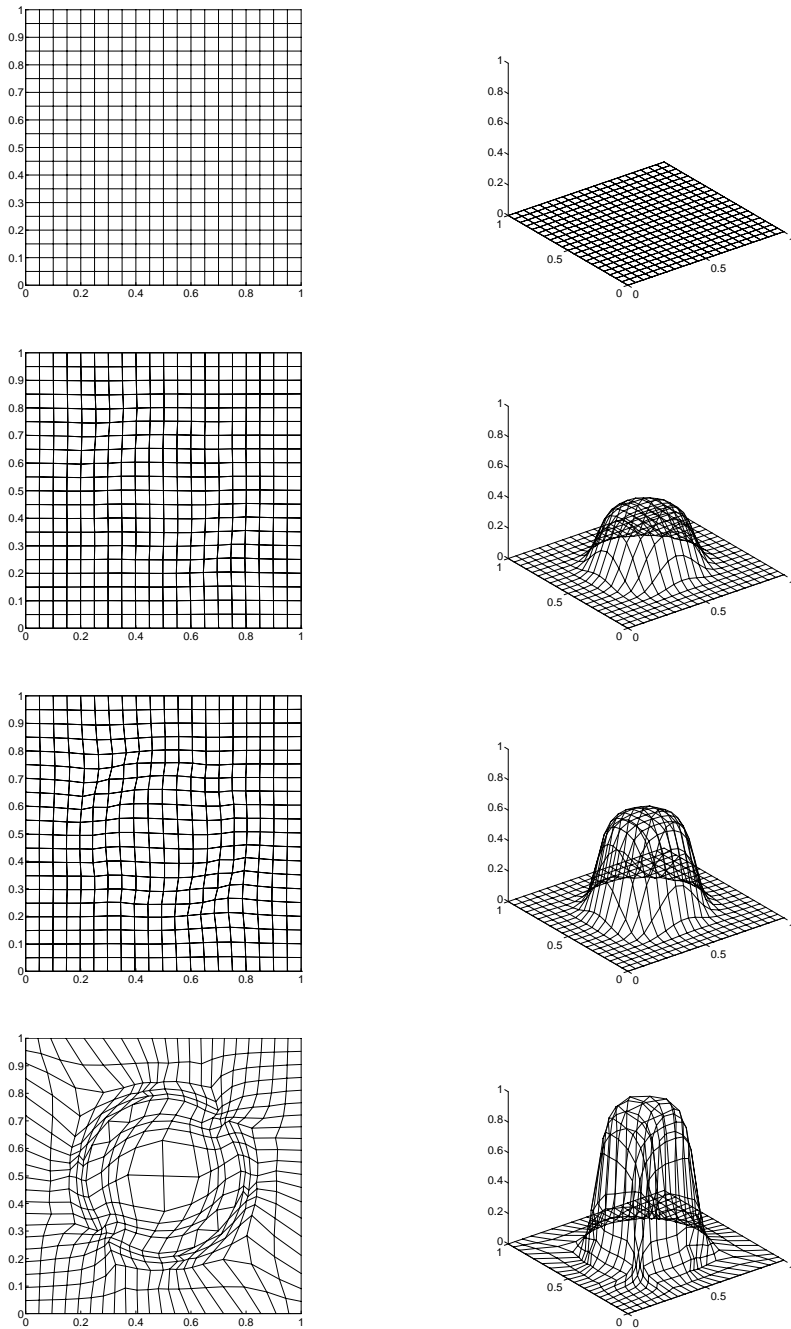


Figure 5: Evolution of grid and solution to steady-state in 2D. Values of θ are 0, 0.5, 1 and 100.

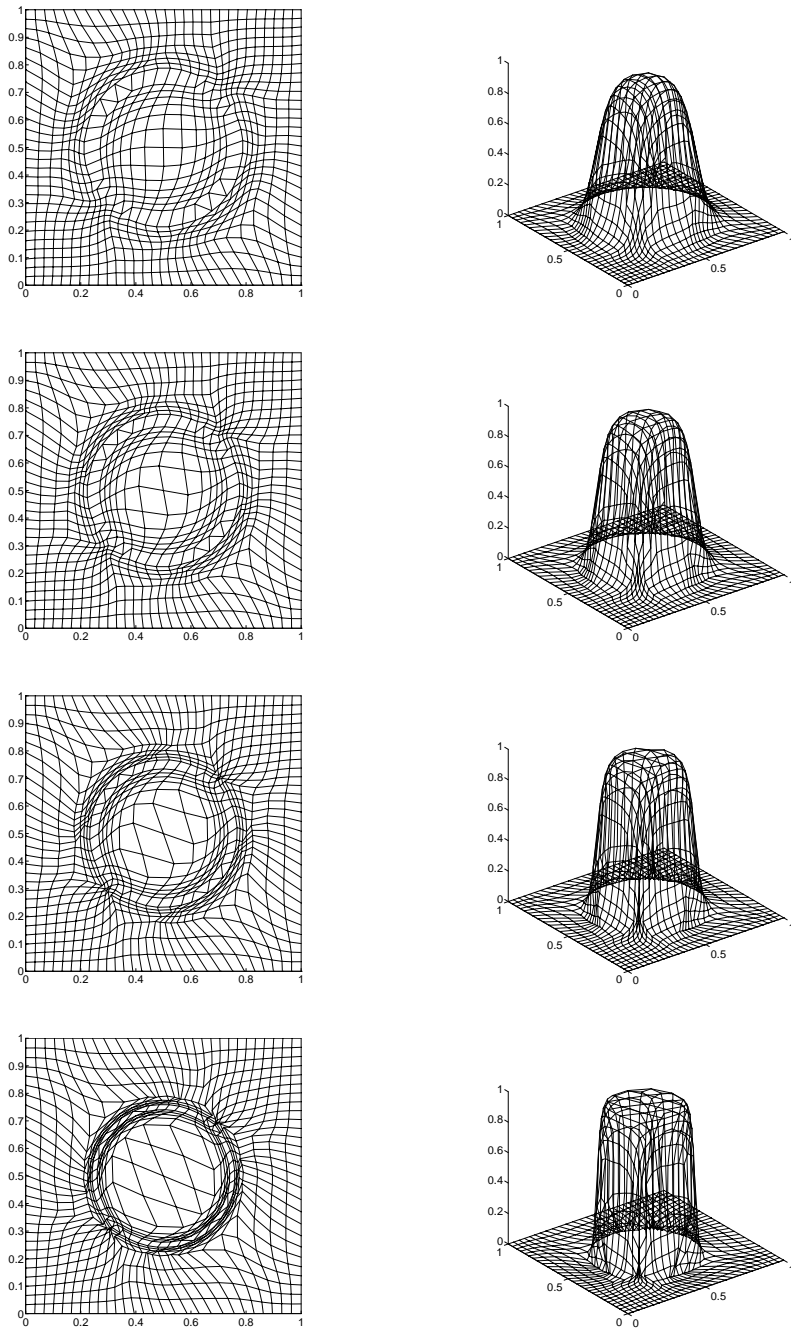


Figure 6: Steady-state grids and solutions for example 2 for increasing values of R .

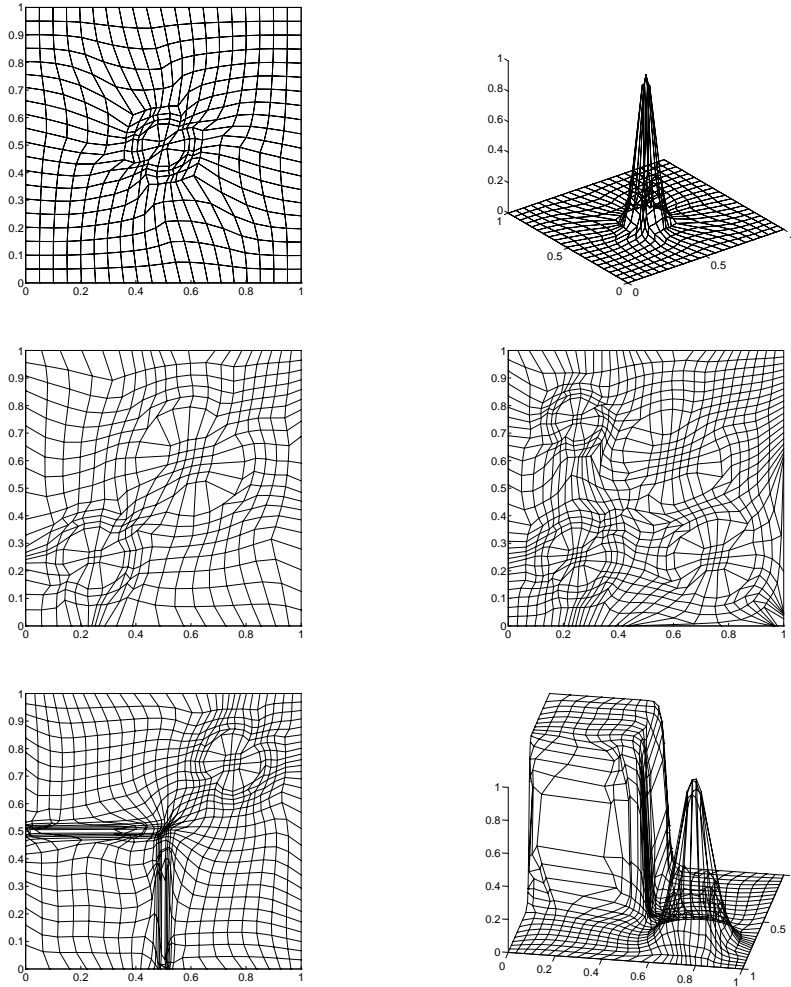


Figure 7: Grid and solution for example 3 (upper two figures); grids and solution for example 4 (lower four figures).

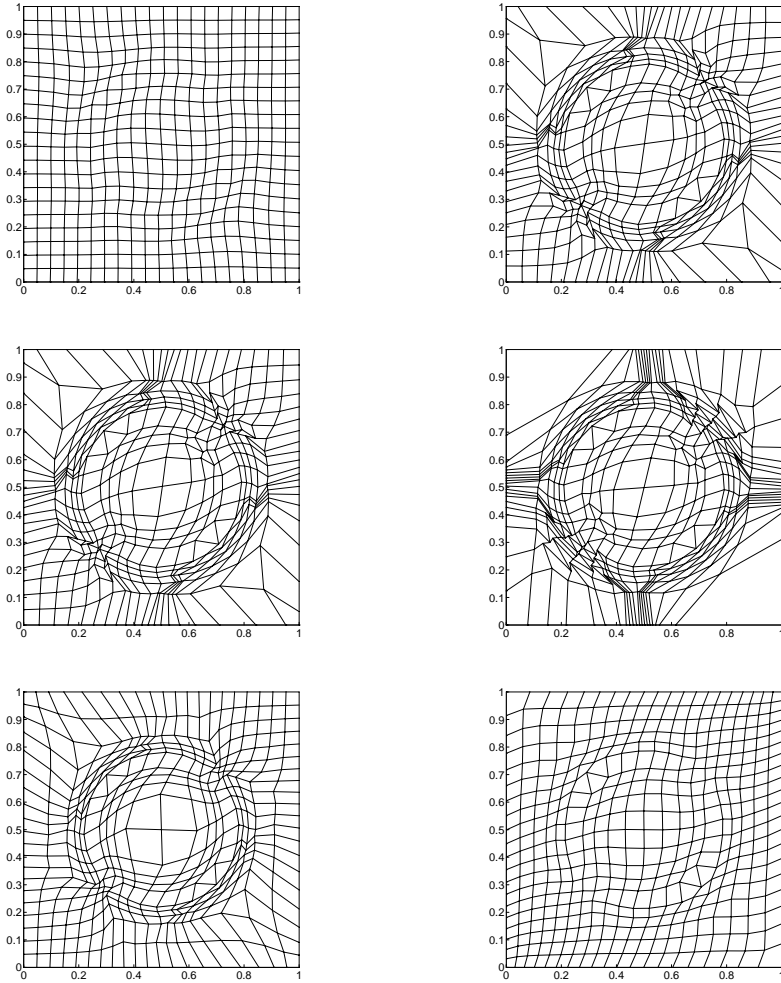


Figure 8: Variation in the method parameters. Upper two figures: δ -variation ($\delta = 0.01$ and $\delta = 10$); middle two figures: ϵ_1^2 -variation ($\epsilon_1^2 = 0.01$ and $\epsilon_1^2 = 10^{-5}$); lower two figures: ϵ_2^2 -variation ($\epsilon_2^2 = 10^{-8}$ and $\epsilon_2^2 = 10^{-5}$).